2012

Characterization of Doped Gallium Nitride Substrates

Jack Lee Owsley III
Wright State University

CHARACTERIZATION OF DOPED GALLIUM NITRIDE SUBSTRATES

A thesis submitted in partial fulfillment of the
requirements for the degree of
Master of Science in Engineering

By

JACK LEE OWSLEY III
B.S. Wright State University, 2010

2012
Wright State University

WRIGHT STATE UNIVERSITY

GRADUATE SCHOOL

December 4, 2012

I HEREBY RECOMMEND THAT THE THESIS PREPARED UNDER MY SUPERVISION BY Jack Lee Owsley III ENTITLED Characterization of Doped Gallium Nitride Substrates BE ACCEPTED IN PARTIAL FULFILLMENT OF THE REQUIREMENTS FOR THE DEGREE OF Master of Science in Engineering.

_____

Elliott Brown, Ph.D.
Thesis Director

_____

Kefu Xue, Ph.D.
Chair, Department of Electrical Engineering

Committee on Final Examination

_____

Elliott Brown, Ph.D.

_____

Jason Deibel, Ph.D.

_____

Bruce Claflin, PhD.

_____

Andrew Hsu, Ph.D.
Dean, Graduate School

ABSTRACT

Owsley III, Jack Lee. M.S.Egr. Department of Electrical Engineering, Wright State University, 2012. Characterization of Doped Gallium Nitride Substrates.

In this thesis the characteristics of five bulk semi-insulated doped gallium nitride samples provided by Kyma Technologies, Inc were explored. The five GaN samples were grown on sapphire substrates by hydride vapor phase epitaxy (HVPE) and doped with different concentrations of iron, hydrogen, carbon, oxygen and silicon. The first step of characterization was measuring the optical absorption of all the samples using a UV-NIR fiber spectrometer. Through this procedure it was found that they all showed a strong absorption at 518 nm. Thus, time-resolved differential transmission measurements were conducted at this wavelength using the second harmonic generation (SHG) of a femtosecond ytterbium-doped fiber amplifier (YDFA), mode-locked laser. Relaxation times between 24 and 433 picoseconds were obtained. Finally, four point probe measurements were performed in the order to determine the bulk resistivity of the GaN samples. The measured values are within the order of $10^6 \Omega$*m for all samples.

Table of Contents

List of Figures

List of Tables

List of Equations

I. INTRODUCTION

Semiconductors are an essential part of the advancement of technology. Since the development of the junction transistor in 1947, semiconductor materials have been implemented into radio frequency and computing devices worldwide. Now thanks to special material development techniques, compounds of specific elements can be created to fit a wide range of applications. Advancements in ultrafast lasers in the last 25 years have made it possible to characterize certain aspects of semiconductors, such as their energy band gaps. To better understand the energy band gaps and other defects, it is clear that photo-carrier relaxation times are one of the properties of interest in semiconductors, which can be extracted by time-resolved differential measurements. This process consists of exciting electrons in the semiconductor and probing their relaxation time using an ultrafast laser.

This project is a collaboration with Kyma Technologies, North Carolina. This company is a major contributor to the advances in the compound semiconductor field including design, fabrication, certain crystal growth techniques and state of the art processing equipment used for fabricating materials. One of their current projects is to create GaN semiconductors that have a relatively short photo-carrier lifetime, on the

order of tens of picoseconds. In hopes to achieve a short photo-carrier lifetime Kyma introduced dopants (iron, hydrogen, carbon oxygen and silicon) into the sample.

This report presents results from different techniques to characterize five doped GaN samples. Kyma's main focus was the inter band electron absorption, so to understand the energy states in the GaN band gap, transmission measurements ranging from 200 nm – 1000 nm were first performed. This UV-NIR transmission measurement is to measure the absorption coefficient caused by the defects and the varying concentration of the dopants in the sample. In a second step, a unique time-resolved differential transmission setup is constructed with an excitation energy that is selected based on the absorption measurements. This experiment uses a high powered ultrafast ytterbium-doped fiber amplifier (YDFA) laser and an intricate optical component design to resolve the photo-carrier relaxation time. It has been requested that the output of the YDFA to be used will be capable of generating four different wavelengths: 1035, 518, 343 and 259nm. Since there is inter band gap absorption present in the samples, Kyma has instructed that we proceed with the second harmonic (518 nm) of the YDFA, since the energy corresponding to 518nm in an inter-band energy for GaN.

Finally, this report presents the bulk resistivity measurements performed on all of the samples. Semiconductors are used in circuitry and other electrical devices, and it is necessary to know the resistivity for certain applications. This is an experiment conducted by using a state of the art Lucas four point probe setup, powered and measured by a Keithley 2400 Sourcemeter.

II. Samples

2.1

Kyma used a process known as hydride vapor phase epitaxy (HPVE) to produce the samples. This process is used to grow thick (≈500μm) GaN layers and successively remove the substrate without damaging the GaN samples. The crystalline structure of the bulk GaN samples needed to be taken into account when considering the substrate on to which they were grown. Sapphire (trigonal crystal system) is a commonly used substrate for this procedure, even though there is a lattice mismatch with GaN (Wurzite type crystalline structure). The lattice difference causes defects which lead to the spontaneous separation of the sample from the substrate after a critical thickness of GaN has been reached. It has been shown that the critical thickness of GaN on sapphire using the HVPE process is near 500 micrometers.

During the growth process, solid ammonium chloride transforms into NH_6 and HCl at temperatures near 900°C. Once decomposed, the NH_6 and HCl react with liquid gallium to form trichloroaminegallium, whose vapor is transported to the substrates by nitrogen gas. Here the $GaCl_6NH_6$ decomposes and forms gallium nitride. When a critical thickness is reached the gallium nitride will spontaneously separate from the sapphire substrate due to the deposition defects. It is common to introduce dopants into the gallium nitride to produce different optical and electrical effects. For Kyma's application, iron, hydrogen, oxygen, silicon and carbon are incorporated as dopants to shorten the

GaN photo-carrier lifetime. Gallium nitride is a commonly used (Binary III-V compound) semiconductor, which has a naturally long recombination time due to its large bang gap energy (3.4eV) (discussed in 2.2). The reason for exploring the capabilities of GaN, in comparison to say GaAs, is because of its durability in applications such as, optoelectronics, high-frequency and high power devices.

Table 1 and Figure 1 display the different samples concentration levels of silicon, hydrogen, oxygen, carbon and iron and the actual samples respectively.

Sample	**Silicon Concentration (66 ^{66})**	**Hydrogen Concentration (66 ^{66})**	**Oxygen Concentration (66 ^{66})**	**Carbon Concentration (66 ^{66})**	**Iron Concentration (66 ^{66})**
AE 2518	7.0 E17	1.6 E18	1.2 E17	4.1 E16	4.5 E17
AE 2522	2.7 E17	1.4 E18	1.4 E17	5.5 E16	8.6 E17
AE 2527	2.5 E17	2.5 E18	6.0 E16	4.7 E16	5.9 E17
AE 2529	2.4 E17	1.5 E18	1.2 E17	8.2 E16	1.8 E18
AE 2057	Unknown	Unknown	Unknown	Unknown	Unknown

Table 1: Dopants concentration levels of the Kyma samples.

Figure 1: The five GaN samples provided by Kyma.

Since the properties of the gallium nitride are different depending on the type and concentration of the dopants, the absorption coefficient must be recorded to determine what wavelength of the laser system will provide enough energy to excite the electrons to the conduction band. If there is not enough energy to excite the electrons to the conduction band then the relaxation time at the experimental wavelength cannot be measured. The absorption coefficient is determined by using a UV-NIR fiber spectrometer.

2.2

When the absorption of the material is understood, one could then deduce the energy (eV) corresponding to any wavelength (λ in m) of interest using a Planck's relation shown in Equation (1).

$$6=\frac{6\times 6}{6} \qquad (1)$$

h= Planck's constant and c= the speed of light in a vacuum.

Semiconductor materials have a specific, known, band-gap energy which can be expressed in electron volts. If the energy band gap is unknown, one can use a spectrometer to determine by measuring the absorption or the transmission of a sample over a large range of wavelengths and thus determine the band gap. The absorption of the light will show that the photons transmit their energy to the material's photo-carriers.

The fiber spectrometer used in this experiment is a StellarNet UV-NIR. A Deuterium/ Tungsten light source produces the wavelengths that are monitored by two separate spectrometers, the Black-COMET (200-1080nm) and the Red-DWARF (900-

1700nm). A stand is used to hold the sample in place and position the light source and spectrometer fibers five millimeters apart from one another. Orienting the source directly above the spectrometer fiber ensures the maximum transmitted power is measured.

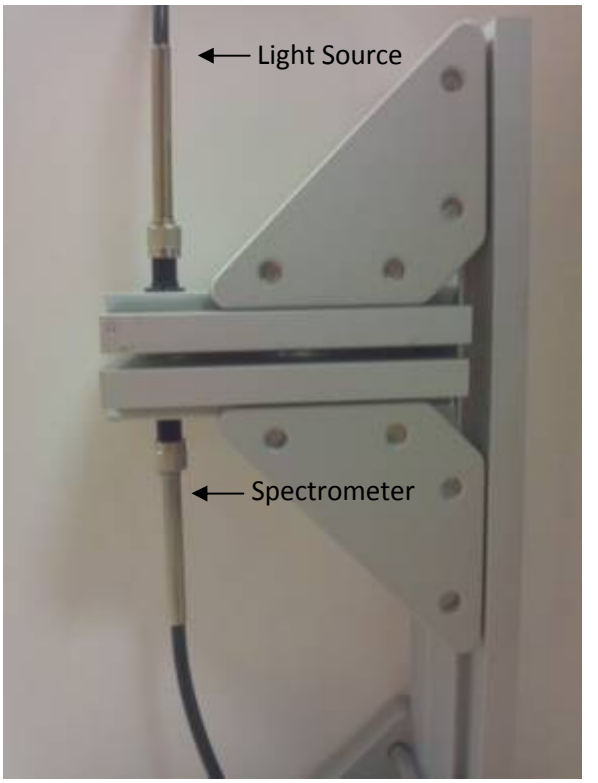

Figure 2: StellarNet transmission stand

2.3

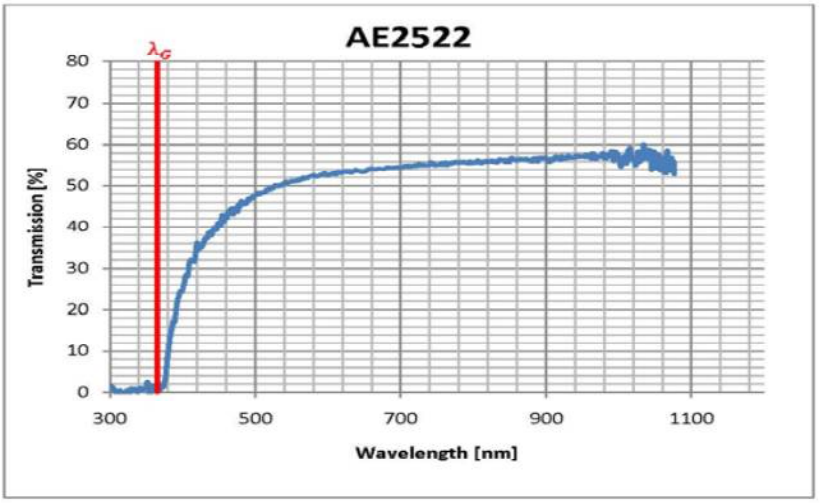

Figure 3:
Transmission for the GaN sample AE2522 using StellarNet spectrometer.

Sample	**AE2518**	**AE2522**	**AE2527**	**AE2529**	**AE2057**
Transmission % at 518 nm	32	50	58	40	53

Table 2: Sample transmission percentage at 518 nm for all of the samples

Figure 3 shows a typical measurement of Kyma's samples obtained with the spectrometer. It is clear that the spectrometer output displays zero transmission below 365nm and an increase in transmission up to 60 % above 365nm. This is because 365 nm is the energy band edge of GaN (3.4 eV≈ 365nm). Since all of the samples have similar transmission patterns, the remaining transmission percentages at 518 nm are listed in Table 1. From these measurements and the understanding that GaN is a direct band

material, the decision to proceed with the inter-band time-resolved differential transmission at 518 nm was made.

III. Time-Resolved Differential Transmission

3.1

Atoms have a different number of electrons from one element to another, and these electrons populate a discrete (single valued) energy level. The energy levels are filled from the level closest to the nucleus outward and in most cases there are not enough electrons present to fill the outer most energy level. The electrons that are present in this outer band are better known as "valence" electrons. The levels that are filled are considered imperturbable, because of their strong bond to the nucleus. The valence electrons however, are bound to the nucleus with a low energy and are the significant entity in the electron excitation process. In a solid structure, the valence electrons are conjoined to the nearest atom by ionic bonding or covalent bonding. The Pauli Exclusion Principle suggests that two fermions cannot occupy the same quantum state simultaneously, leaving two electrons with opposite spins to form each energy level. The energy levels stack atop one another resulting in the valence band. When a high enough external energy source is applied to the semiconductor (this specific energy will be discussed), the covalent bonds can be broken, causing the electrons to wander throughout the lattice and making the material conductive. Once this bond has been broken, there are subsequently spaces where the electrons once were, which are called holes. Now the freed electrons can be considered to have been excited from the valence band to the conduction band. The amount of energy needed for this excitation depends on the energy gap between the two bands or the energy "band gap". Also one must take into

consideration the concept of direct and in-direct band gaps in semiconductor material. This is where either the momentum of the holes and electrons are the same or different in the material respectively. If the momentums are different, then a portion of the electron momentum is transferred to the lattice structure of the material, but if the momentums are the same, then the material will emit a photon.

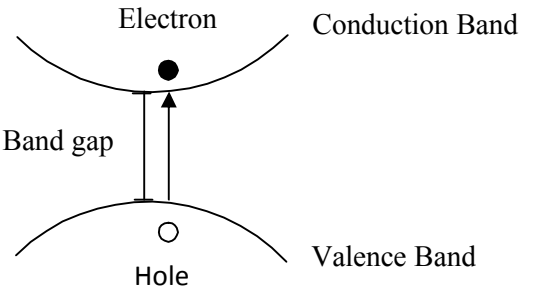

Figure 4: Typical band structure
for a direct band gap

When a semiconductor is doped, the substance will occupy the host's lattice sites randomly throughout the semiconductor. Purposefully experimenters will select this dopant so that the newly formed semiconductor has extra holes or electrons. When the dopant contributes electrons to the semiconductor, it is called a donor. A semiconductor doped with donors has more electrons than holes. A semiconductor doped with acceptors has more holes than electrons. Donors and acceptors have specific energy levels that will lie within the band gap of the semiconductor; the dopant can be many different materials as long as its energy band gap is lower than that of the semiconductor. Meaning the dopant energy level will be present in the energy band gap of the host semiconductor.

After donor and acceptor levels have been considered, it is important to establish whether the material satisfies the intrinsic or extrinsic conditions. When a material is said to have a dominating intrinsic region, the carrier concentration is determined primarily by the inter-band transitions. The general approximation of the electrons (n) and holes (p) is

$$n = p \qquad (2)$$

From [12] it is found that the intrinsic concentration (n_6) can be compared to the concentration of donors (N_6) and acceptors (N_6) to verify if the intrinsic conditions are met by Equation (3).

$$n_6 \gg (N_6 - N_6) \qquad (3)$$

The difference between the two electron concentrations is the available carriers to be excited from the donor level to the conduction band. When Equation (3) is true the impurities left after the difference in the concentration levels is determined will not influence the electrons that are excited from the valance band, and the sample is thought of as pure.

Materials with a dominating extrinsic region have contributing impurities that have carriers which will exceed the carriers provided by the inter-band excitation. There are two different types of extrinsic regions, and the first of which is when the donor concentration is higher than that of the acceptor $N_6 \gg N_6$ and when the acceptor concentration is higher than the donor $N_6 \gg N_6$. If the material is extrinsic, the intrinsic and extrinsic fields are compared as such:

$$n_6 \ll N_6 \qquad (4)$$

or

$$n_6 \ll N_6 \qquad (5)$$

Since this project involves substrates that are highly doped with five different dopants, it is safe to assume that our measurements will be in the extrinsic region of the material. Taking advantage of the advances in deep level transient spectroscopy (DLTS) [14][15] and Hall Effect experiments, it can be determined that the levels are donors or acceptors and their inter-band depth. Once the inter-band structure in understood, the photo-carrier lifetime becomes a material characteristic of interest.

A time-resolved differential transmission (TRΔT) setup is used to measure the photo-carrier relaxation time of a semiconductor. This experiment is based on a two-step process. First, a high power optical pulse (pump) is focused on the semiconductor. This first pulse excites the electrons from the valence band of the semiconductor to the conduction band. Then a second pulse, delayed in time with respect to the pump pulse is called the probe, and it is used to measure the differential transmission. The energy of the probe beam has to be about ten times smaller than the energy of the pump beam; this is to be sure the probe pulse does not modify the absorption. From this procedure the experiment is also known as "pump-probing". In pump-probe experiments the necessary laser pulse duration depends on the relaxation time of the electron in the material. For example, here the laser pulse is 150 femtoseconds, but the relaxation time is on the order of picoseconds. Shorter pulse durations give a smaller measurement resolution of the signal step size [10] and [12] .

This experiment can be modeled mathematically. As a first step the excitation is treated as an instantaneous process, meaning the excitation has relatively no rise time [11]. If this is done and the relaxation g_6 is assumed to be mono-exponential with a recombination lifetime τ, then the two are related by:

$$g_6(t) = u(t)[A_6 e^{\frac{6\,6}{6}}] \qquad (6)$$

with 6_6 being the amplitude of the detected signal and u(t) being the unit step function which will allow $g_6(t)$ to increase instantaneously from 0 to 1 at t=0 (t<0 u(t)= 0; t>0 u(t)=1). This model is useful in the understanding and estimating the relaxation time, but instantaneous excitation is impossible. Because of the finite pulsed laser rise time, the pump pulse width will create a small electron rise time. A pump pulse with a pulse width σ of a mode-locked laser used in a degenerate pump-probe setup is given as:

$$p_{666\,6}(t) = p_{66666}(t) = B \times \exp(\frac{6\,6^6}{6^6}) \times \sin(2\pi v_6 t) \qquad (7)$$

v_6 is the center frequency of the laser, B is the detected signal amplitude and the $p_{666\,6}(t)$ and $p_{66666}(t)$ are the pump and probe pulses as a function of time. A degenerate pump-probe setup is where the pump and the probe are of the same wavelength. It is necessary to realize the instantaneous excitation from before must be modified to a mathematical equation that will include the finite time of the electron excitation, shown in Equation (4).

$$g_6(t) = \int_{6666}^{6} g_6(Y) \times p_{666\,6}(Y - t)dY \qquad (8)$$

This convolution between the instantaneous time domain signal and the pump pulse now models a true mathematical representation of the excitation of the electron in a semiconductor. Furthermore, as the time resolved differential transmission (TRΔT) measurement is made, another convolution between the pump and probe pulses overlap is

exercised. This is a necessity because the probe pulse has the same induced dynamic effects as the pump pulse on the sample and will modify the measured results. The overlap is model as:

$$g_6(t) = \int_{6666}^{6} g_6(X) \times p_{66666}(X - t)dX \qquad (9)$$

$$= \int_{6666}^{6} g_6(Y)[\int_{6666}^{6} p_{6666}(Y - X) \times p_{66666}(X - t)dX]dY \qquad (10)$$

Also using the pump and probe beam pulses we can generate an autocorrelation. Autocorrelation is the cross correlation of a signal with itself and is used to find repeated patterns in a signal. The temporal overlap of the pump and probe pulses given by Equations 7-10

$$C(\tau) = \int_{6666}^{6} p_{6666}(Z) \times p_{66666}(Z - \tau)\, dZ \quad (11)$$

$$= \int_{6666}^{6} B\exp 6\frac{66^6}{6^6}6 \times B\exp 6\frac{6(666)^6}{6^6}6\, dZ \quad (12)$$

$$= B^6 \exp\left(\frac{66^6}{66^6}\right) \qquad (13)$$

$$= C_6 \exp\left(\frac{66^6}{6^6}\right) \qquad (14)$$

with $w = \sigma\sqrt{2}$ being the width of the Gaussian autocorrelation function. The autocorrelation can be measured independently using two-photon absorption in a semiconductor diode or using second harmonic generation in a thin nonlinear material. From this we can calculate the actual measured signal:

$$g_6(t) = \int_{6666}^{6} g_6(Y) \times C(Y - t)dY \qquad (15)$$

The true detected signal can be extracted if the instantaneous excitation expressed in Equation (6) and the Gaussian pulses from Equation (10) were substituted into Equation (15), which is demonstrated in Equation (16). The optical pulse, ideal response and the

real response are all shown in Figure (5). Notice how a small rise time is monitored in the real response compared to the ideal "spontaneous" response.

$$g_6(t) = C_6 \int_{6\,6\,6}^{6} [A_6 \exp(\frac{6\,6^6}{6_6{}^6})] \times \exp(\frac{6\,(6\,6\,6)^6}{6\;^6})\, dY \quad (16)$$

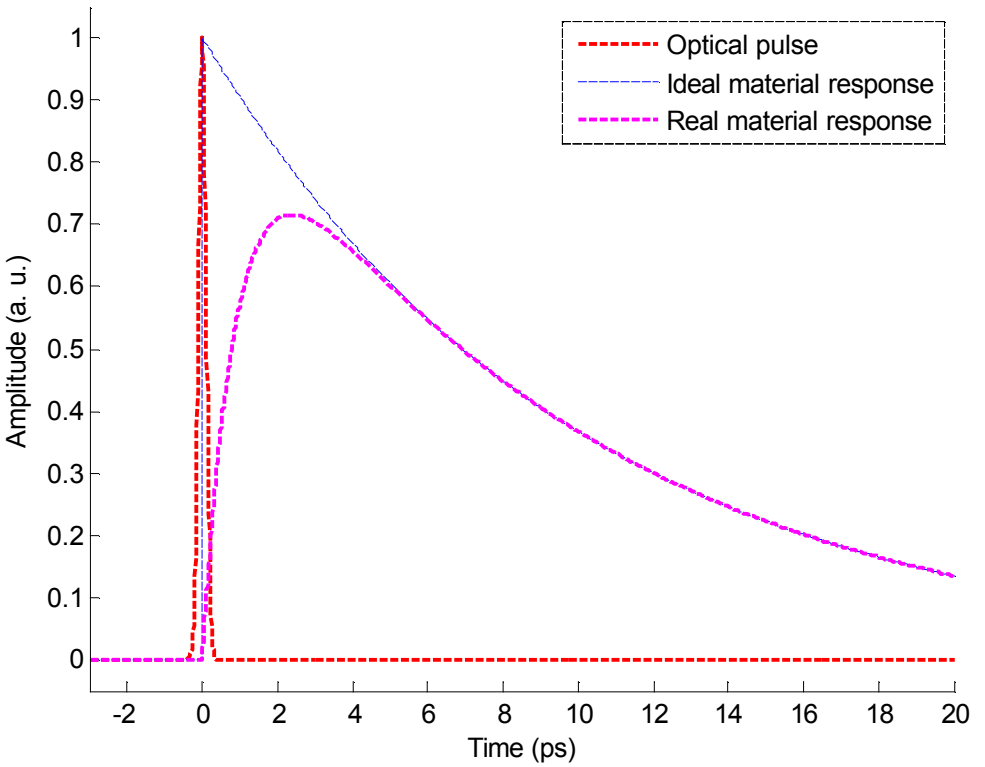

Figure 5: Optical pulse, ideal material and real material responses with $\tau = 10$ and $\sigma = 0.1$

There are three main recombination types that are of consideration for this experiment:

- Radiative recombination: this is a direct recombination between an electron from the conduction band and a hole from the valence band. After the recombination, energy is given off in the form of a photon.

- Schockley Read Hall Recombination: this recombination is performed through defect levels where dopants in the semiconductor create energy levels in the energy band gap which can trap electrons from the conduction band. The trap will hold the carrier until it is thermally reemitted into the conduction band or until its carrier counterpart moves to the same trapping level, and in this case the two recombine.
- The Auger recombination: this is a non radiative process involving more than one electron. An excited electron transfers its energy to another electron before recombining with a hole. This three particle interaction is not easily produced because it is only significant in non-equilibrium conditions.

3.2

The laser used in the (TRΔT) experiment is an ultrafast high power Ytterbium-Doped Fiber Amplifier Mode Locked Laser (YDFA MLL). This is a class IV mode-locked laser with a 1.171 W average output power at the fundamental wavelength (1035 nm). The fundamental wavelength's polarization is vertical (for this experiment, the polarization will not make a difference).The repetition rate is 31.1034 MHz with a pulse width of 150 fs, shown in Figure (6). The fundamental output of the laser is connected to an external optical harmonic generation box via a fiber cable. This box is capable of generating four harmonics derived from the fundamental wavelength: 1035 nm (1.171 W), 518 nm (163 mW), 344 nm (18.3 mW) and 259 nm (52.26 mW).

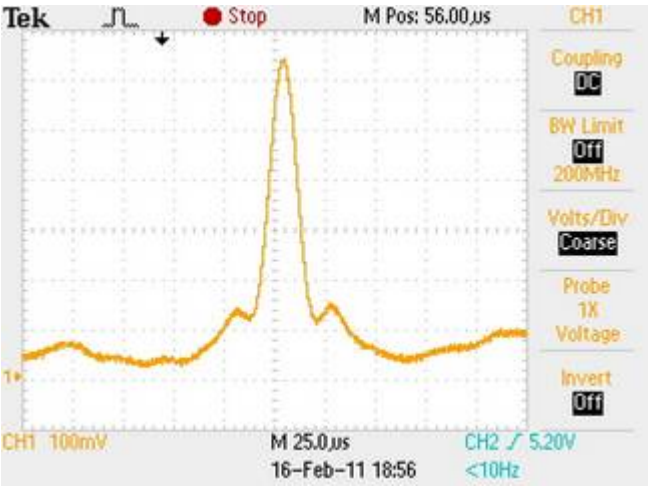

(a)

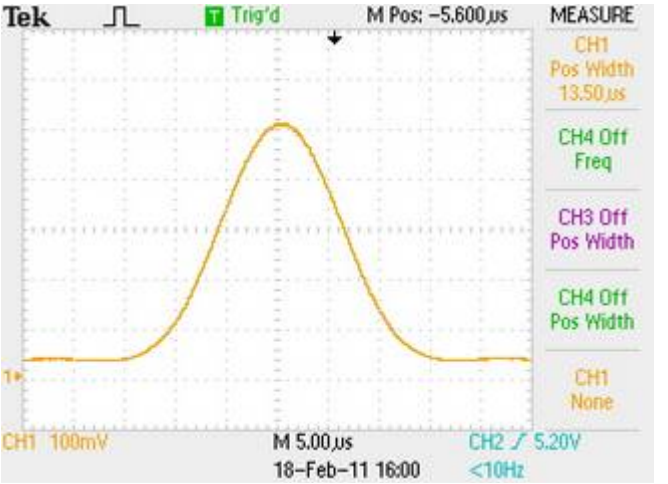

(b)

Figure 6: Autocorrelations of the fundamental (a) and SHG (b).

Firgure 7: YDFA harmonic generations (right box) with pump-probe setup (left).

Thanks to its high power and the provided wavelengths, this laser meets the experimental requirements, which has been expressed in Chapter 2. Unfortunately, because of the unique set up of the optics, not all of the outputs of the harmonics are located on the same side of the box, meaning the SHG (518 nm) was on the opposite side of the fundamental wavelength (1030 nm), THG (344 nm) and FHG (259 nm). Since one would want access to the most outputs as possible, it was found that either multiple outputs were to be sacrificed or the needed experimental wavelength would be inaccessible. After specific power/wavelength analysis, it was discovered that the THG contained high power leakage of the fundamental and second harmonic generations. However by using specific filters, it was found that one could block the fundamental and the third harmonic to only transmit the SHG with a power of 157mW. Thorlabs filters FGB37 and FGL435 were used and their individual optical transmissions are shown in Figure 8(a). It was possible to use a single filter to achieve the same filtering effect, but

such filters are generally expensive, and the attenuated power was sufficient with the double filtering technique, displayed in Figures 8a and 8b.

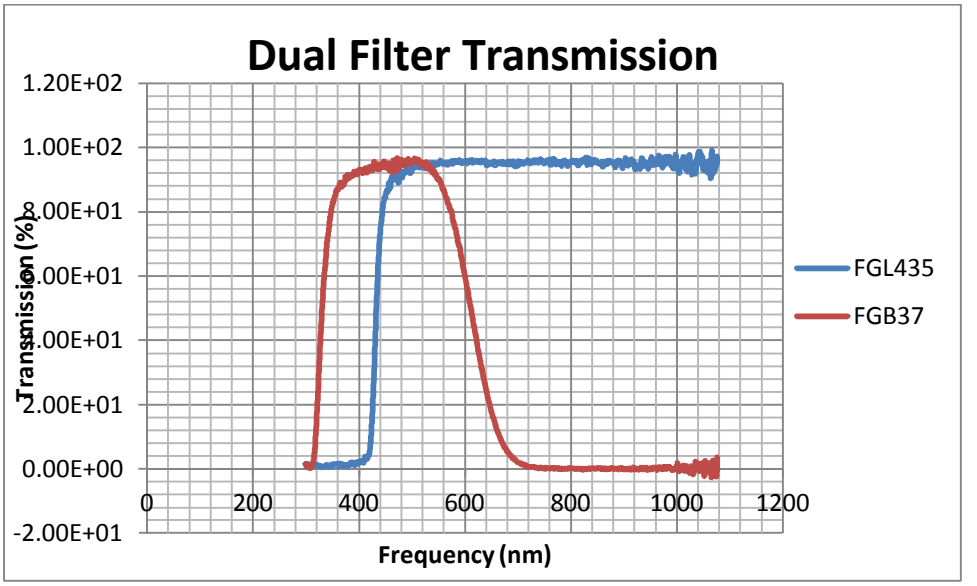

(a)

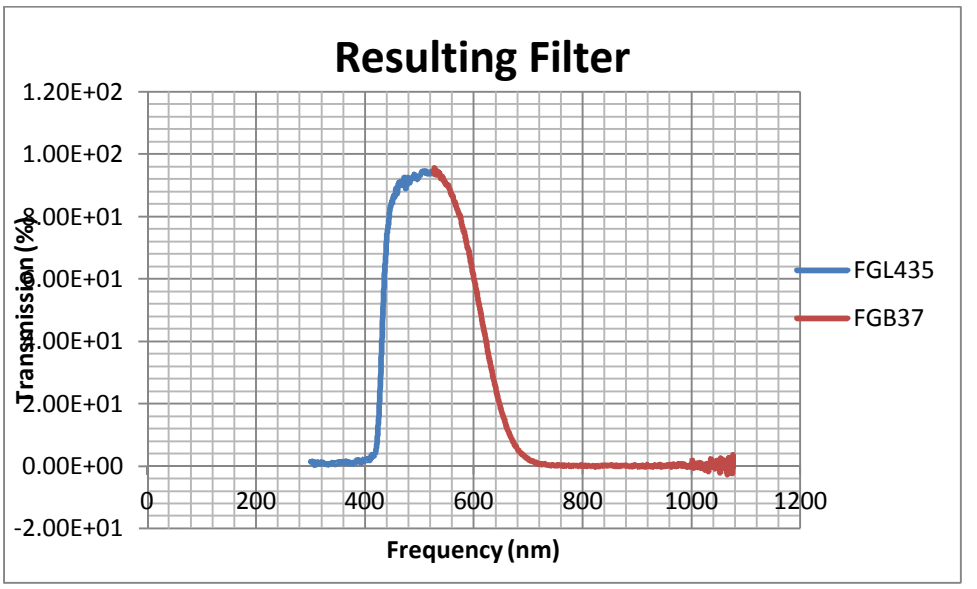

(b)

Figure 8:
(a)Transmission of the dual filter system and (b) Resultant of dual filter system.

To realize a time-resolved differential transmission setup, a few criteria have to be respected. The basic limitations and necessities are the same throughout all pump-probe configurations, but there is freedom for one to manipulate the setup to their advantage, for example our filters. The requirements after the beam-splitter split the pump and probe beams are:

- Both of the pump and probe pulses must take the same amount of time to travel from the beam-splitter to the sample. This is because the pump and probe pulses must be able to overlap in time.
- The pump beam power must be about ten times higher than the probe beam power to ensure the probe does not modify the absorption.
- There needs to be a delay-line. A time delay is necessary to tune the delay between the probe pulse and pump pulse so that one can achieve a time resolved measurement as well as sweep the probe pulse.
- An optical chopper must be placed in the pump beam path.

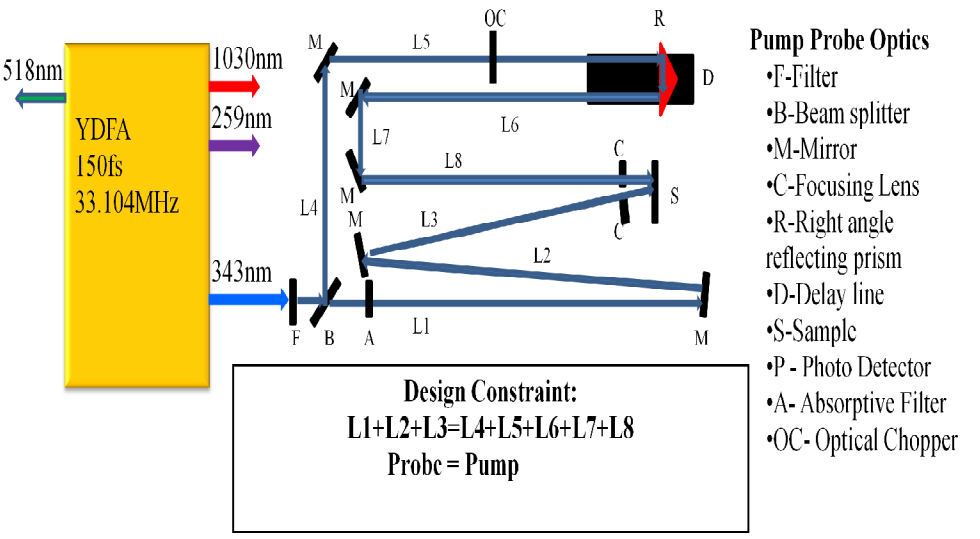

Figure 9: Block diagram of YDFA pump-probe setup.

The photo-carrier lifetime of the sample can be graphed after the pump and probe pulses have overlapped. Obviously all semiconductors have different photo-carrier lifetimes, so it is necessary to use a delay-line with a range longer than the expected photo-carrier lifetime. The delay-line imposes the maximum range of the measurement and a sampling oscilloscope can be used to observe the overlapping of the two pulses. Also the step size of the delay-line increases the measured signal's resolution and the length of the temporal window.

The pump pulse is used to "bleach" the sample. Bleaching a semiconductor is to say making the sample "transparent" at a wavelength by exciting all of the electrons located in the valence band and make them fill all of the available states in the conduction band for this very energy. When the pump beam is focused on the sample, there is a creation of electron-hole pairs and they recombine until another pump pulse comes. Since there are no photo-detectors that are fast enough to directly resolve such a fast effect, is impossible to directly measure the effect. So in order to overcome these two constraints, a delay-line combined with an optical chopper is commonly used. The optical chopper is set in the pump beam path and modulates the optical beam at a known frequency (around 400Hz). When the pump pulse reaches the sample, the semiconductor will be transparent at this wavelength (when there is no delay between the pump and the probe pulses), and consequently the probe pulse will pass through the sample. When the pump pulse is blocked by the optical chopper, the semiconductor is absorbent, thus the probe beam will be absorbed. As a result, the probe beam, which carries the time-resolved differential transmission, is modulated at the same frequency as the chopped

pump beam, but with opposite phase. In doing this, one would place a detector behind the sample as to receive the transmitted probe pulse and neglect the pump beam signal. When the beams are focused at the same spot, the probe pulse will either be permitted to be transmitted (when pump beam is present), or denied (when pump beam is blocked by the chopper). While the pump beam is being chopped and the detector receiving the probe pulse signal, the delay line is used as somewhat of a sampling device. Increasing step by step, the time delay between the pump and the probe pulses could be as little as tens of picoseconds when using a sampling oscilloscope. Once the initial pump pulse position is found, the delay-line is set in motion to overlap the probe pulse onto the pump pulse, allowing the detector to receive the excitation and relaxation of the electrons. Both chopper and detector are connected to a Stanford lock-in amplifier, the chopper producing the reference frequency and the detector providing the detected signal. The lock-in will then resolve the differential transmission data.

Our specific time- resolved differential transmission setup is unique in many different ways, starting with our beam-splitter. It is expensive and hard to meet the correct specifications needed in a pump-probe process when selecting the beam-splitter at 518nm. To overcome this situation a 70/30 splitting ratio was used, then adding a Thorlabs NE10A absorptive filter to the probe beam. This particular filter has near 10% transmission at 518nm. The reason for necessarily low probe beam transmission is due to the attenuation caused by the presence of the chopper in the pump beam path, which creates a 3dB loss. After the attenuation system, the probe beam is simply redirected by Thorlabs aluminum mirrors and then focused on the sample with a plano-convex lens. Figures 10 depicts the setup of the TRΔT at 518nm. Also we delayed the pump pulse

instead of the probe pulse for stability reasons and to guarantee consitent probe pulse readings.

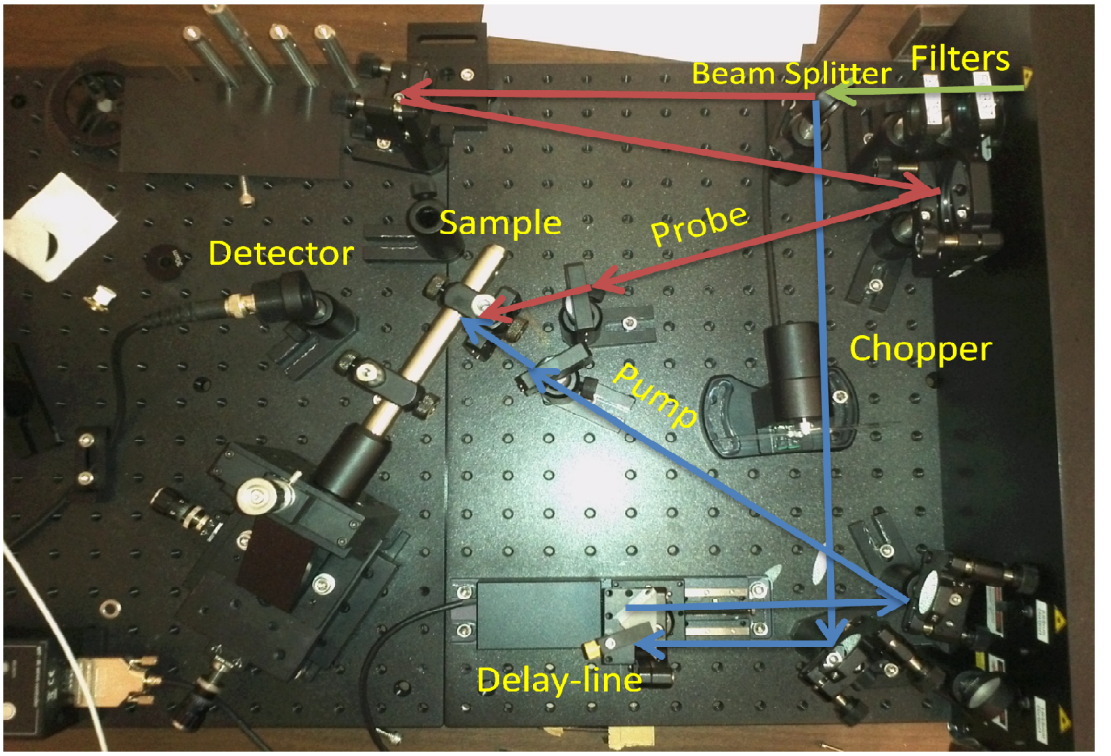

Figure 10: Actual pump-probe design.

The pump beam was redirected by a mirror onto a right angle prism reflector, which made the optical component of our delay line. The delay line was initially driven by a 50mm Thorlabs translation stage. After multiple runs, the wobble on the driving screw of the translation stage was so great the pump beam was not providing a consistent illumination on the sample and its range was not long enough for some of the GaN samples. It was consequently decided to purchase a new translation stage from Zaber, Figure 11. The new stage is 100mm long with an incremental movement of ≈47nm

(0.282 femtoseconds). This delay-line is good enough to ensure the pump beam intensity is consistent and the complete lifetime is measured.

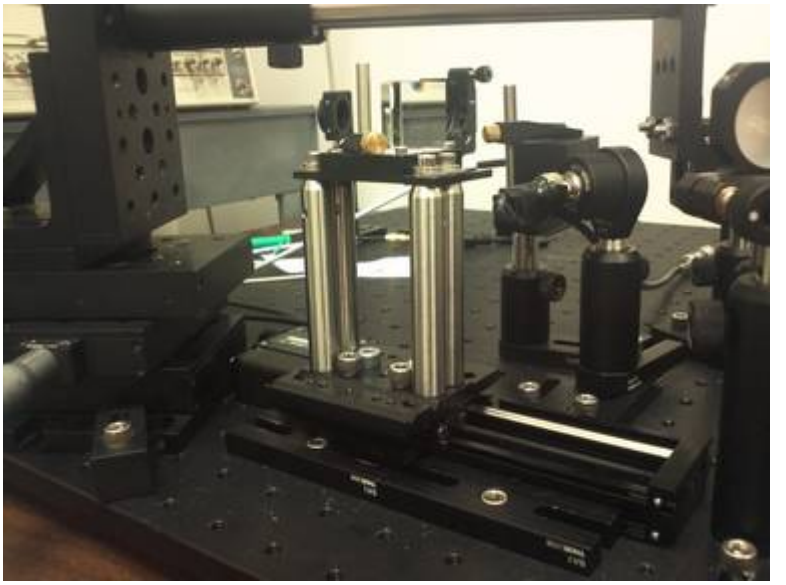

Figure 11: Delay line. Shown: Zaber 100mm translation stage, one inch right angle reflector and custom stand

After the beam is aligned through the right angle prism, it was focused onto the sample, but not before an optical chopper was incorporated in the path. Here, a Thorlabs optical chopper was used with a MC1F10 (ten slot) blade. It was necessary to use this blade because the chopper system is designed to designate the modulation frequency according to the number of slots on the blade. The desired modulation frequency was a high prime number to ensure that the detected signal at this frequency was the modulated signal and not harmonics produced by the power supply (for example).

Now when the beams were aligned on the sample, it was necessary to use a pinhole to make certain the beams were overlapping at a single point on the sample within a margin of the pinhole's diameter. There was a variety of pinholes used for alignment, ranging from 100µm-15µm. The larger pinholes were used for a rough estimate to get the beams in a general proximity of one another, and the smaller pinholes

were used for higher accuracy. Once the beams were overlapped, because of the small diameter of the pinhole, they were focused on to a Thorlabs high speed photo detector (Model: SV2; rise/fall time 150ps) which was coupled through a SMA connection to a Tektronix sampling oscilloscope. A screen display of the Tektronix oscilloscope when the delay line was tested is shown in Figure 12.

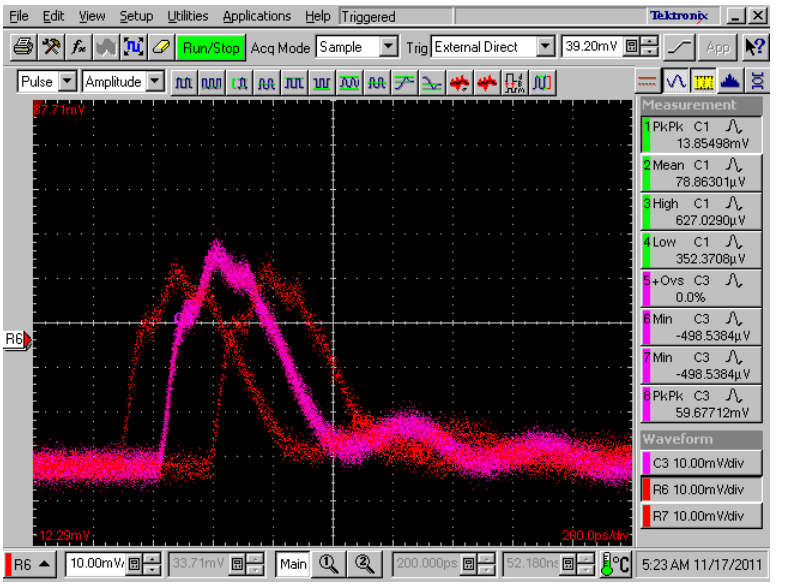

Figure 12: (Right red) Pump pulse initial position, (Left red) Pump pulse final position and (Pink) Probe pulse.

The photodiode was positioned exactly where the sample would be. This trick permits one to measure the delay difference between the pump and the probe pulses. This is useful to confirm that the zero degree overlap is located within the delay-line range and that the position of the delay-line is correct for long relaxation measurement. After confirming that the pump and probe beam paths were the same in time and the delay line zero degree overlap position was correct in the range of the delay-line, it was possible to incorporate the sample at the beam overlap position. Once the sample was in

position, we placed a Thorlabs photodiode (SM1PD2A; rise/fall time 45ns) on the backside of the sample so as to measure the probe beam. The pump beam has to be avoided since only the probe pulse is carrying the differential transmission. If the pump beam was detected, the probe pulse would be flooded into the pump beam signal. The setup now uses the chopper and delay-line manipulation as discussed before.

Lock-In amplifiers are utilized to measure and detect very small alternating current (AC) signals (as small as nanovolts). A method known as phase-sensitive detection (PSD) is used to single out the element of the signal at a specific reference frequency and phase (PSD). Since a lock-in amplifier requires a reference frequency to detect an experimental excitation, the PSD permits the amplifier to amplify the detected signal and multiply it by the lock in reference, (Equations (17) and (18)).

$$V_{6\,66} = V_{666}V_6 \times \sin(\omega_6 t + \theta_{666}) \quad (17)$$

$$= \frac{6}{6}V_{666}V_6 \cos 6[\omega_6 - \omega_6]t + \theta_{666} - \theta_{6666} - \frac{6}{6}V_{666}V_6 \cos 6[\omega_6 - \omega_6]t + \theta_{666} - \theta_{6666}6 \quad (18)$$

where $V_{6\,66}$ is the PSD signal amplitude, V_{666} is the signal amplitude, V_6 lock-in reference amplitude, $\omega_6$and ω_6 are the angular frequencies of the signal and lock-in respectfully and θ_{666} and θ_{666} are the phases of the signal and lock-in respectfully.

Furthermore, if the ω_6 equals ω_6 then the measured output will be a DC signal proportional to the signal amplitude, shown in Equation (19).

$$V_{6\,66} = \frac{6}{6}V_{666}V_6 \cos(\theta_{666} - \theta_{666}) \quad (19)$$

The PSD process allows the lock-in amplifier used (SR810), the ability to detect a signal with a bandwidth as low as 0.01Hz. In order to get the data from the lock-in amplifier, a Prologix GPIB-USB controller reads the digital output of the lock-in-amplifier and transmits it to a unique LabView program. This program plotted the detected signal by

the photodiode in real time, which allowed the user to have full control of the project. This specific LabView program also allowed the user to determine the direction of the scan (backwards and forwards) as well as the step size, scan range and the averaging time for each point. A typical signal plot from the LabView program is presented as Figure (13). This is the screenshot of the relaxation time of the Kyma sample AE2522.

3.3

Here are the findings of the time-resolved differential transmission experiment for all five of the samples. There is extra information of a sample AE2524 that was of interest in the beginning of the project, but was later turned down. Its information is shown to show transmission consistency throughout the samples.

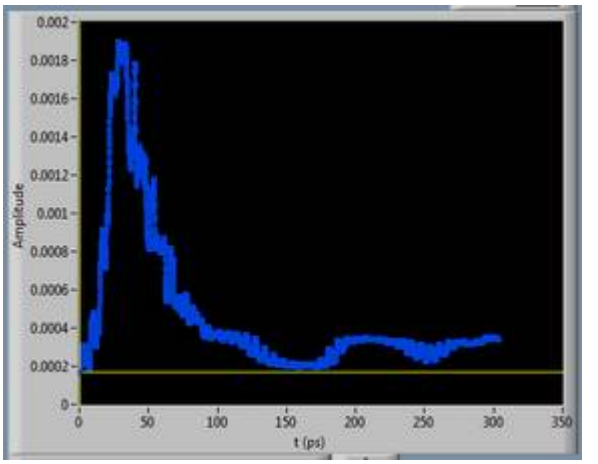

Figure 13: LabView output of the electron-carrier relaxation time.

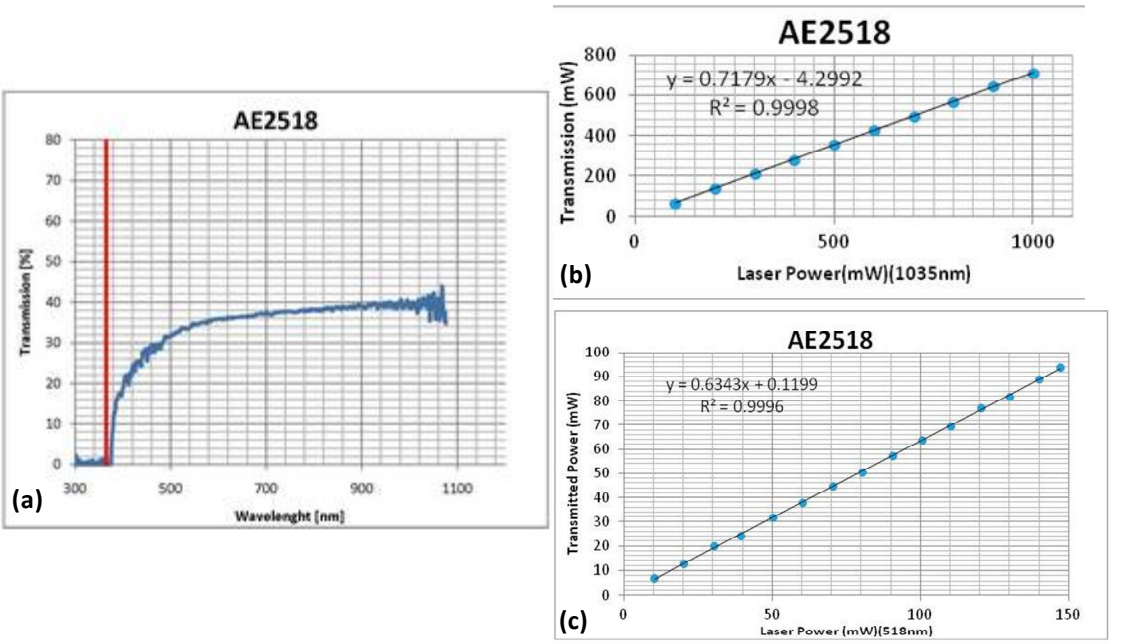

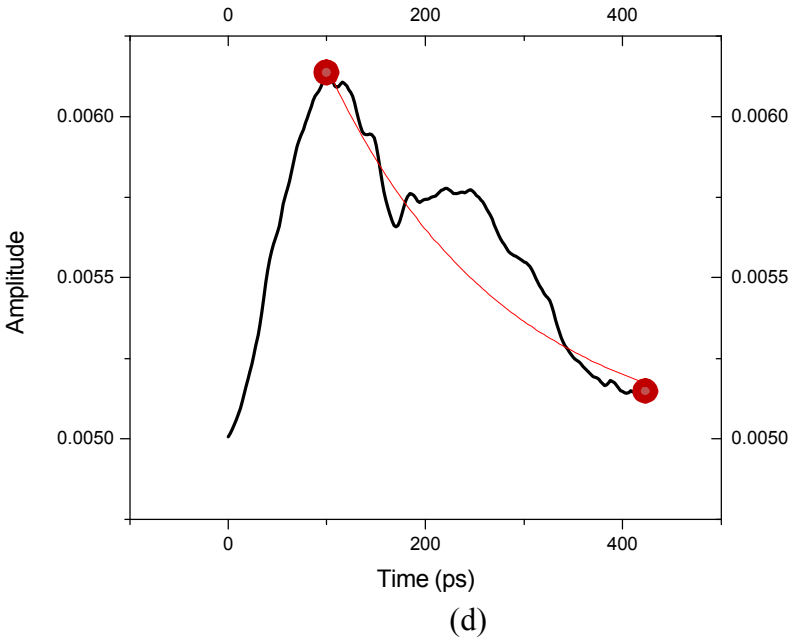

(d)

Figure 14: Transmission characteristics of sample AE2518 measured by: (a) UV-VIS-IR fiber spectrometer, (b) YDFA at 1035 nm, (c) SHG of YDFA at 518 nm and (d) Origin carrier lifetime measurement.

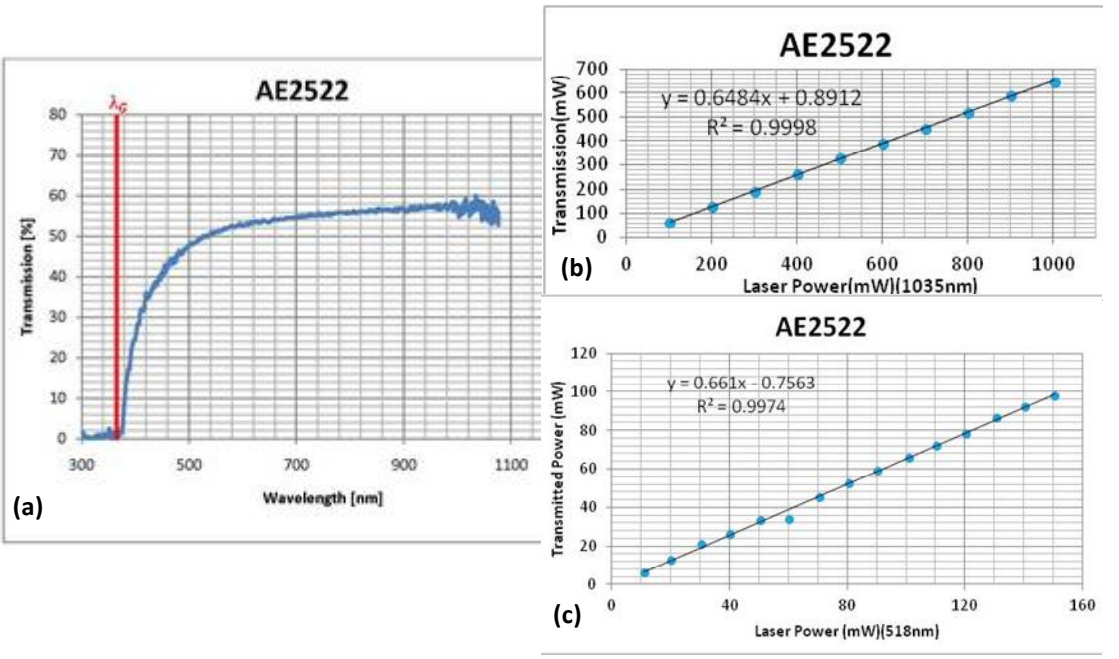

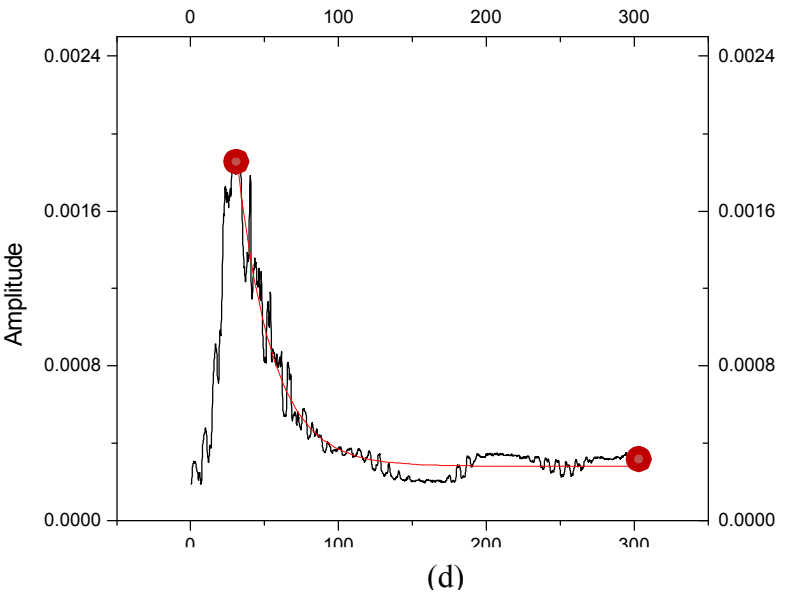

Figure 15: Transmission characteristics of sample AE2522 measured by: (a) UV-VIS-IR fiber spectrometer, (b) YDFA at 1035 nm, (c) SHG of YDFA at 518 nm and (d) Origin carrier lifetime measurement.

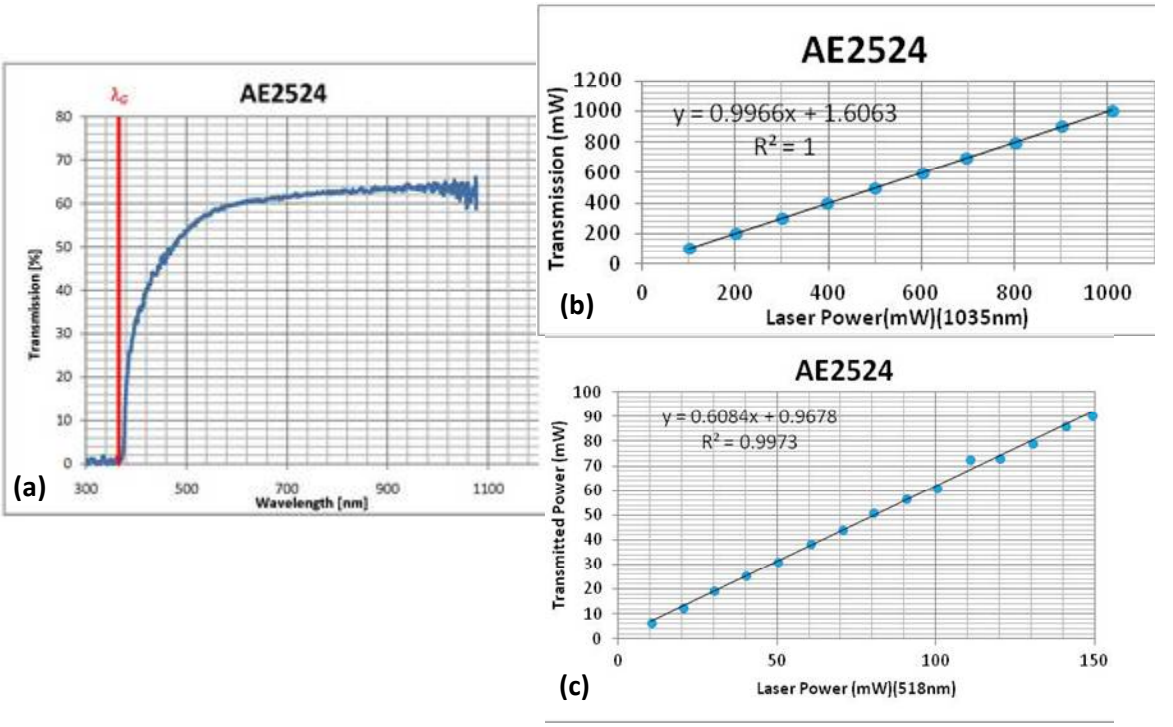

Figure 16: Transmission characteristics of sample AE2524 measured by: (a) UV-VIS-IR fiber spectrometer, (b) YDFA at 1035 nm and (c) SHG of YDFA at 518 nm.

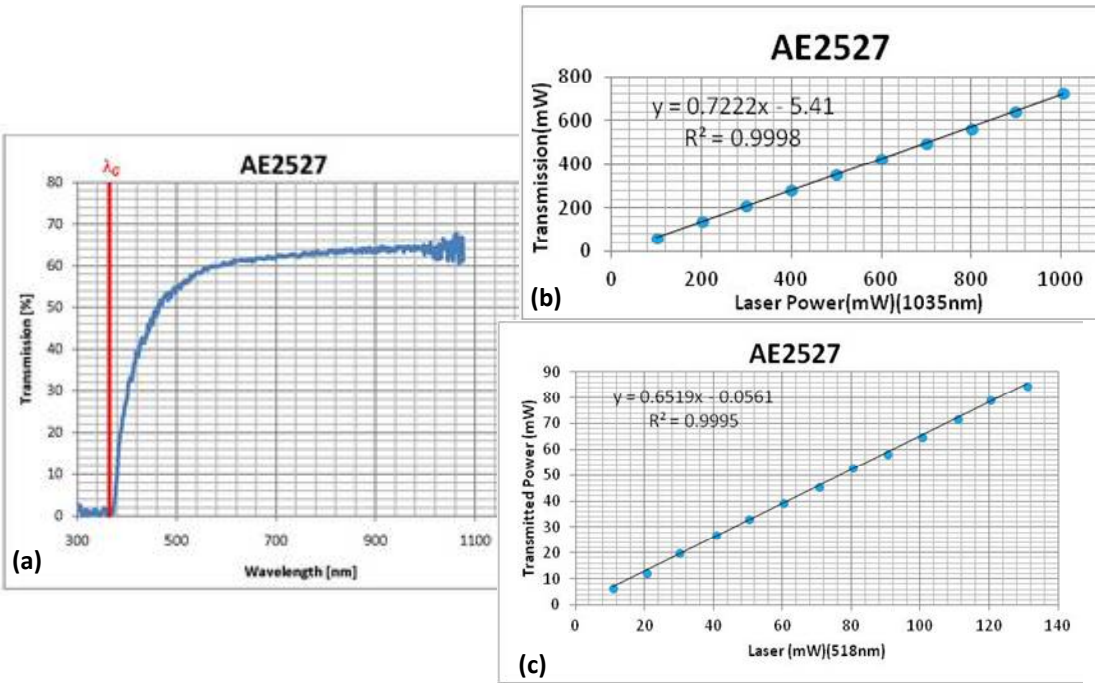

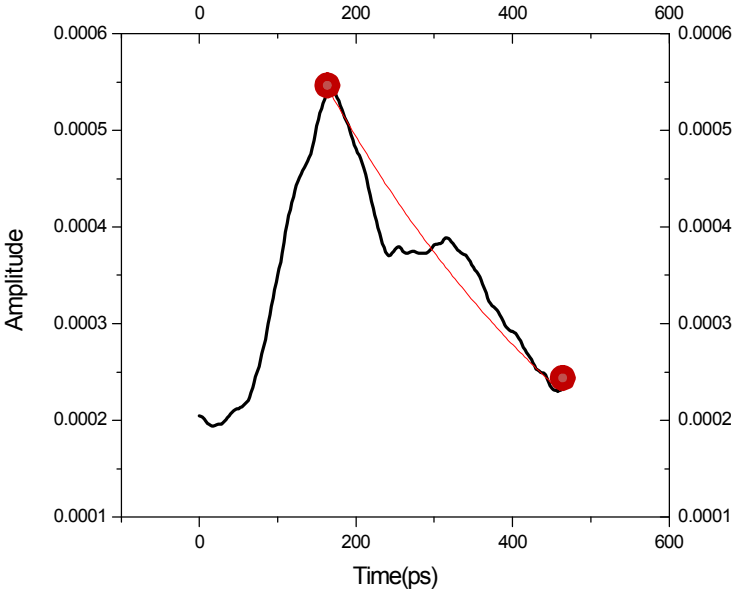

(d)

Figure 17: Transmission characteristics of sample AE2527 measured by: (a) UV-VIS-IR fiber spectrometer, (b) YDFA at 1035 nm, (c) SHG of YDFA at 518 nm and (d) Origin carrier lifetime measurement.

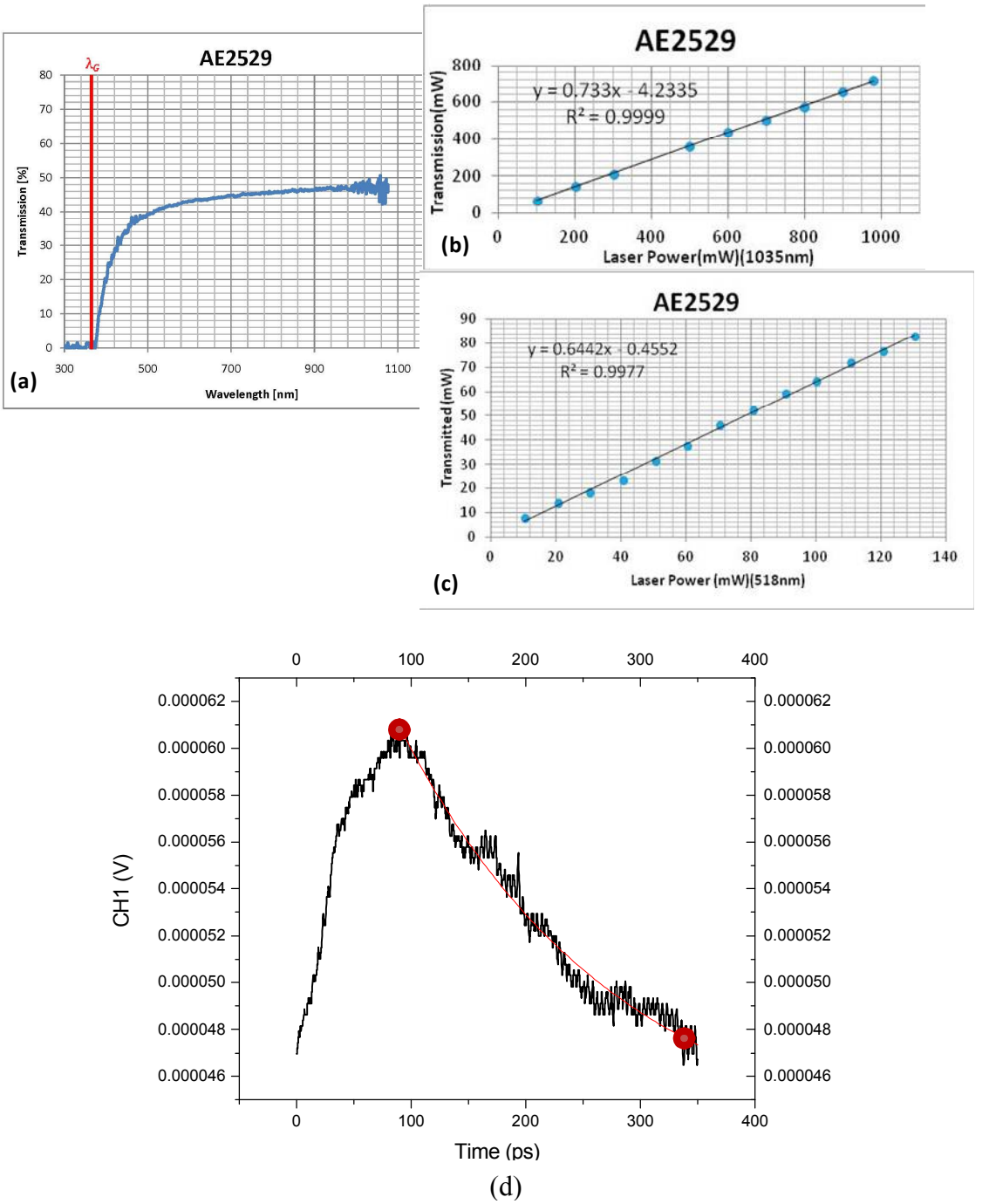

Figure 18: Transmission characteristics of sample AE2529 measured by: (a) UV-VIS-IR fiber spectrometer, (b) YDFA at 1035 nm, (c) SHG of YDFA at 518 nm and (d) Origin carrier lifetime measurement.

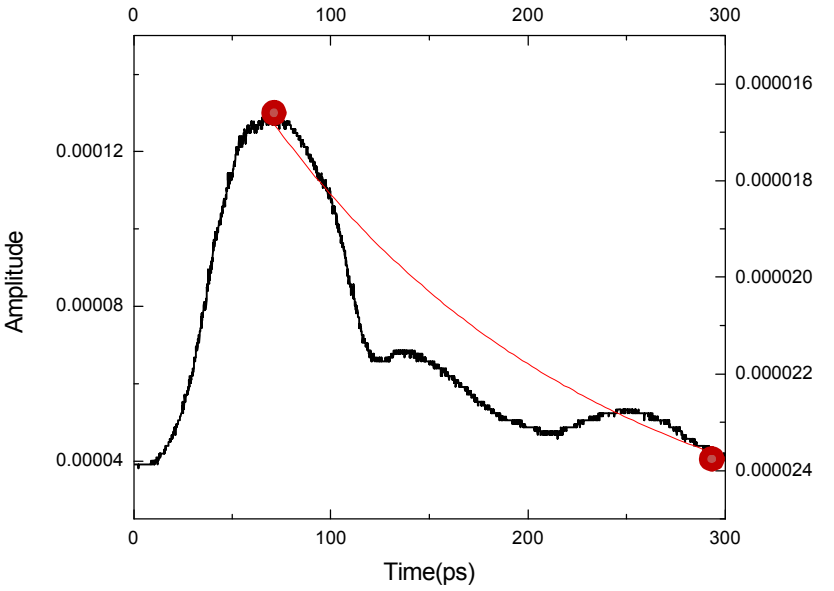

(c)

Figure 19: (a) Pump-probe photo-transmission measurement from Sample AE2057, (b) Pump-probe photo-transmission measurement from sample AE2057 (second run) and (c) Origin carrier lifetime measurement.

Sample	**Silicon Concentration (66 [66])**	**Hydrogen Concentration (66 [66])**	**Oxygen Concentration (66 [66])**	**Carbon Concentration (66 [66])**	**Iron Concentration (66 [66])**	**Lifetime (ps)**
AE 2518	7.0 E17	1.6 E18	1.2 E17	4.1 E16	4.5 E17	180
AE 2522	2.7 E17	1.4 E18	1.4 E17	5.5 E16	8.6 E17	24
AE 2527	2.5 E17	2.5 E18	6.0 E16	4.7 E16	5.9 E17	433
AE 2529	2.4 E17	1.5 E18	1.2 E17	8.2 E16	1.8 E18	190
AE 2057	Unknown	Unknown	Unknown	Unknown	Unknown	167

Table 3: Dopants concentration levels of the Kyma samples with lifetime measurements.

3.4

Since there a known amount of dopants incorporated into the gallium nitride substrates, it is a safe assumption that the samples will experience a recombination through defect levels (SRH). This is supported by what we have mentioned concerning the dopants but also by the measured absorption during the UV-NIR experiment (chapter II). This absorption was measured below the known gallium nitride energy band gap (3.4 eV), which would refer to a defect level. Also by process of elimination we can rule out radiative recombination since the material did not show signs of emission. Furthermore we could rule out Auger recombination because this effect is negligible.

The measurements recorded and repeated are very interesting, starting with the fact that the relaxations measured do not return to the amplitude in which they began which is an expected characteristic in a traditional TRΔT experiment. Also they do not follow the usual bi or mono-exponential shape, the traditional relaxation time form. Each one of the samples relaxation times are unique in shape and display a wide range of relaxation time. The differences in shapes have been discussed and possible conclusions have been drawn. For example, the plateau from ~250nm – 350nm could be a temporary trapping effect during the electron-hole recombination/relaxation time. But, it also has been argued that the slight increase of amplitude in the graph near 350nm could be a re-excitation of the electrons from the trap levels to the conduction band. To justify the probability of this being the case, one could either know the donor and acceptor levels of the dopants and substrate or perform other tests to extract this information. The most important test would be to perform Hall measurements on the samples. By executing this

experiment, we would be able to measure the difference in Hall voltages which would give a clearer picture to what type of a semiconductor (p or n) we have present. Also the intensity of the Hall voltage would display how drastic the difference between the amount of acceptors and donors. Also, by carrying out a deep-level transient spectroscopy experiment (DLTS) beneficial in determining if there are defect levels that would contribute to the unique photo-carrier relaxation patterns.

IV. Sheet Resistivity

4.1

Resistivity is the electrical property of a material that determines the materials ability to resist current flow over a certain area and is another parameter of interest in the field of semiconductors. Since semiconductors are used in circuitry and other electrical devices, it is necessary to know the bulk resistivity. To acquire this information we will be carrying through an experiment known as the four-point probe method. This is the method of placing four probes directly in contact with the sample, with the two outer probes will carry a constant electrical current through the sample and the two inner probes will measure a voltage. Contrary to the outdated two point probe method, four point probing is exposed to a negligible amount of voltage drop across the sensing wires, which is preferred. For low resistive material, it is clear the current would have to at a higher setting than high resistive material, but one must keep in mind heating effect caused by the current

4.2

The bulk resistivity of the five samples is measured. This is done by sweeping a current using the four point probe setup and measuring the output voltage. Using Equation 16 the samples' bulk resistivity is calculated under the condition the distance between the probes is known. Below in Figure 20 is a diagram of a basic four point probe experiment. $\pm$ I are the source currents, $\pm$ V are the measured voltages, s is the

probe spacing, 6_6 and 6_6 determine the limits for integration and the sample is the material to be measured.

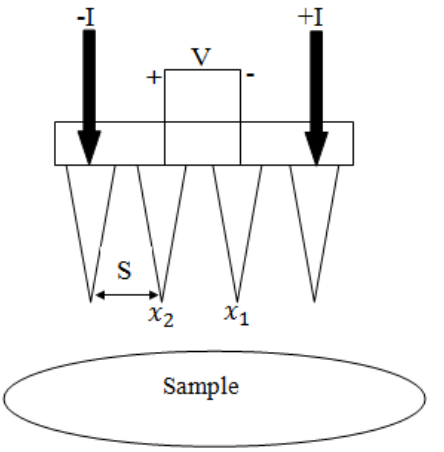

Figure 20: Four point probe setup

First, the assumption of spherical protrusion of the current by the current applying probes (outer probes) is made. From this we form the Equation for the differential resistance, shown in Equation 20.

$$\Delta R = \rho(\frac{66}{6}) \quad (20)$$

where ρ is bulk resistivity, A is area and ΔR is the differential resistance. From Equation 21 we can solve the resistivity by integrating over the distance between these two probes (x_6 and x_6) and because of superposition at the outer probes we obtain an expression for bulk resistivity, displayed in Equation 22

$$R = \int_{6_6}^{6_6} \rho \times \frac{66}{666^6} = \frac{6}{66}(\frac{6}{66}) \quad (21)$$

$$\rho_{6\,6\,6} = 2\pi s \times (\frac{6}{6}) \qquad (22)$$

To measure the resistivity of the samples we use a Lucas- Signatone Pro4 stage and a Keithley 2400 Sourcemeter. First we place the sample on the measurement stage and lower the four point probes until contact is made with the sample. Next a LabView program is designed to allow the user to control the sweep current range and the compliance voltage of the Sourcemeter. Once the parameters are set, the program is executed and the source current and output voltages are recorded and stored. Also the program plots the I-V curve and allows the user to build equations involving the recorded data. This is used to calculate the bulk resistivity of all five samples.

4.3

The compliance voltage set in the LabView program is set to 20V and the source current range is from 0-1μA. These numbers are determined after multiple runs, but once a tolerable current range is found, the samples produce a common I-V curve, shown in Figure 21. After the curves are found to be consistent, data collection began. Next, the average voltage and current for each sample is used with the bulk resistivity equation to produce Table (4).

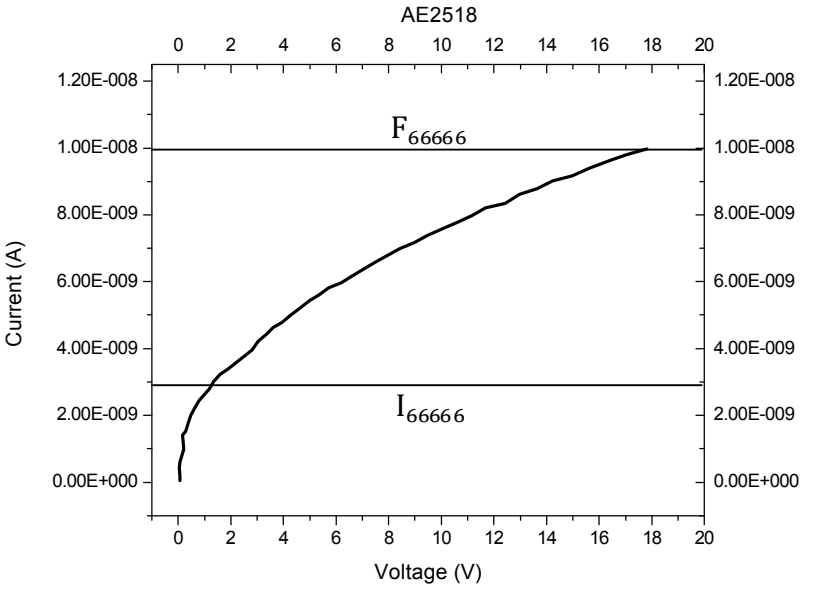

Figure 21: Typical sample I-V curve form

Sample	**AE 2518 Ω-m**	**AE 2522 Ω-m**	**AE 2527 Ω-m**	**AE 2529 Ω-m**	**AE 2057 Ω-m**
Bulk Resistivity	7.85×10^{6}	8.11×10^{6}	8.19×10^{6}	7.92×10^{6}	7.86×10^{6}

Table 4: Sample bulk resistivity

The data collected seems consistent with general GaN characteristics. Gallium nitride has been known to have a linear Current vs. Voltage plot with somewhat of a logarithmic initial response. For consistency, resistivity measurements were only taken between 3×10^{66} and 1×10^{66}, shown in Figure 21 labeled I_{66666} and F_{66666}. This is to ensure that only the linear section of every measured resistivity is included and not the

logarithmic. With the information gathered from Kyma and relevant sources to confirm, the bulk resistivity data measured appears feasible [13].

V. Conclusion

The goal of this project was to optically and electrically characterize five doped gallium nitride samples. This was to be carried out by first analyzing the samples using a UV-NIR fiber spectrometer in order to establish the absorption coefficient for each sample. Then it was necessary to construct a pump-probe setup and measure the relaxation time. Lastly, we measured the bulk resistivity using a four point probe setup.

There was success in obtaining the spectrum of the samples using the UV-NIR fiber spectrometer. It was unnecessary to model the samples' spectrum from ultraviolet into the near infrared since we were to conduct the pump-probe measurements at 518 nm. Each sample showed some type of absorption, which all have been recorded.

A time-resolved differential transmission experiment has been carried out using an ultrafast high powered ytterbium-doped fiber amplifier mode-lock laser. All of the samples relaxation times have been recorded and displayed. Some of the relaxation times are unique in the sense that they have an unusual relaxation pattern. Some possible explanations have been discussed, but the distinctive patterns have not clearly been explained.

There were some problems initially with the pump-probe setup. First, the laser had to be sent back to the manufacturer three times during the course of the project. This was a major setback in the project, and did not grant us much time to work with the

samples. Also the translation stage initially used in for the time-delay had to be changed in the middle of testing due to oscillations created by the driving screw. The wobble of the driving screw over time became more violent and caused an alignment issue with the pump beam. A new translation stage that had virtually no wobble and a smaller step size than the original was then incorporated in the setup.

The resistivity measurements of all five samples have been recorded using a Lucas four point probe stage and a Keithley 2400 Sourcemeter. Initially the experiment experienced some programming setbacks. MATLab was the primary coding language desired for the Keithley 2400, but did not output the I-V curves properly as well as the resistivity calculation. During the time spent rewriting the code, a LabView program was introduced and was able to produce the appropriate information.

If this time-resolved differential transmission experiment were to be carried out again a few things would need to be altered. Looking at the sample relaxations displayed, it is noticeable that most of them do not return to zero. This may be seen if a longer time delay is used. Also the PolarOnyx YDFA would need to be exchanged for a more stable and consistent laser. More than half of the project time was wasted of repair time spent on the YDFA. This is because the high powered ultrafast YDFA is a newer system, but for pump-probe high power is not necessary. Furthermore, if more data was giving on the samples, such as the known resistivity, developmental procedures, the reasoning behind the specific concentration levels, etc. we could better evaluate the gallium nitride samples and the data recorded throughout the entire project.

IV. References

1. Prazmowska, J. et al., (2008). Properties of GaN layers deposited on (0001) sapphire templates. *International Students and Young Scientists Workshop,* , 64-67.
2. Red'kin, A.N., Tatsii, V.I., Makovei, Z.I., Gruzintsev, A.N., & Yakimov, E.E. (2004). Chemical Vapor Deposition of GaN from Gallium and Ammonium Chloride. *40*(10), 1049-1053.
3. Heitz, R., Maxim, P., Eckey, L., Thurian, P., Hoffmann, A., & Broser, I. (1997). Excited states of Fe^3+ in GaN. *Physical Review B, 55*(7), 4382-4387.
4. Wahl, U., Vantomme, A., & Langouche, G. (2001). Direct evidence for implanted Fe on substitutional Ga sites in GaN.*Applied Physics Letters, 78*(21), 3217-3219.
5. Ashraf, H., Kudawiec, R., Misiewics, J., & Hageman, P. (2009). Bulk Growth of GaN by HVPE. *CS MANTECH Conference,* .
6. Gladkov, P et al.. (2012). Below band-gap optical absorption and photoluminescence excitation spectroscopy at room temperature in low-defect-density bulk GaN:Fe. *Applied Physics Letters, 100*(3).
7. Gladkov, P et al.. (2010). Effect ofFedopingonopticalpropertiesoffreestandingsemi-insulating HVPE GaN:Fe. *Journal of Crystal Growth,* , 1205-1209.
8. Sullivan, J.S., & Stanley, J.R. (2008). Wide Bandgap Extrinsic Photoconductive Switches. *IEEE, 36*(5), 2528-2532.

9. Pierret, Robert F.. *Semiconductor Fundmentals*. 1988. Reprint. Reading: Addison-Wesley Publishing Company, 1989. Print.
10. Streetman, Ben G., and Sanjay Banerjee.*Solid state electronic devices*. 6th ed. Upper Saddle River, N.J.: Pearson/Prentice Hall, 2006. Print.
11. Prasankumar, Rohit P.. "Ultrafast Pump-Probe Spectroscopy." *Optical techniques for solid-state materials characterization*. Boca Raton: CRC Press, 2011. 329-370. Print.
12. Omar, M. Ali. *Elementary solid state physics: principles and applications.* revised ed. India (India): Pearson Education, 2004. Print.
13. "Kyma Technologies - Kyma Announces New Conductive and Semi-Insulating GaN Template Products." *Kyma Technologies - Home*. N.p., n.d. Web. 28 Nov. 2012. <http://www.kymatech.com/news/86-kyma-announces-new-conductive-and-semi-insulating-gan-template-products>.
14. Fang, Z., Claflin, B., Look, D., Elhamri, S., Smith, H., Mitchel, W., et al. (2008). Deep centers in semi-insulating Fe-doped native GaN substrates grown by hydride vapour phase epitaxy. *physica status solidi (c)*, *5*(6), 1508-1511.
15. Fang, Z. (2010). Deep traps in AlGaN/GaN heterostructures studied by deep level transient spectroscopy: Effect of carbon concentration in GaN buffer layers. *Journal of Applied Physics*, *108*, 1-3.